Hindawi
Advances in Civil Engineering
Volume 2022, Article ID 5372501, 17 pages
https://doi.org/10.1155/2022/5372501

Research Article

Self-Healing Effect of Various Capsule-Core Materials on Asphalt Materials

Suhua Chen,[1] **Qi Liu**,[1] **Yanqiu Bi**,[2] **Bin Yu**,[1] **and Jiupeng Zhang**[3]

[1]*School of Transportation, Southeast University, Nanjing, Jiangsu 211189, China*
[2]*School of Civil Engineering, Chongqing Jiaotong University, Chongqing 400074, China*
[3]*School of Highway, Chang'an University, Xi'an, Shaanxi 710064, China*

Correspondence should be addressed to Qi Liu; liuqi_@seu.edu.cn and Bin Yu; yb@seu.edu.cn

Received 12 October 2022; Revised 6 November 2022; Accepted 28 November 2022; Published 7 December 2022

Academic Editor: Yuqing Zhang

To further investigate the self-healing mechanism of microcapsules and exclude the interference of capsule-wall materials, a bi-plate test and a molecular model of asphalt and capsule-core materials were established using dynamic shear rheometer (DSR) and molecular dynamic (MD) simulation. Firstly, the models of asphalt-rejuvenator-asphalt and asphalt-epoxy resin-asphalt were established to simulate the interface of asphalt and capsule-core materials. The cross-linking between poxy resin and curing agent, and tensile tests were then simulated through Perl scripts. Finally, the bi-plate DSR test was applied to reveal the different action mechanisms between core materials and asphalt materials. The results showed that the cohesive energy of the epoxy resin and asphalt is greater than that of the rejuvenator at the same simulation time. Meanwhile, the maximum stresses generated after stretching for the two models were 69.9 and 34.68 MPa, respectively. The healing indexes HI_1 and HI_2 have a sound linear correlation with the maintenance time. The HI_1 value of the epoxy resin is greater than that of the rejuvenator, and the maximum value exceeds 1. This implies that the capsule core of epoxy resin can recover the strength of damaged asphalt in a short time. Epoxy resin should be considered for asphalt cracks caused by heavy-load shear.

1. Introduction

During the service life of roadway, traffic loading and temperature cycling may cause asphalt pavement cracking [1, 2]. After cracks appear, moisture damage of asphalt concrete may occur under the repeated action of the load and rain [3]. Self-healing microcapsule materials could be used in the asphalt pavement to improve its self-repairing ability [4]. In recent years, functional materials with self-healing and self-repairing capabilities have been developed [5–7].

At present, the research on self-healing asphalt concrete based on microcapsule has focused on the preparation of microcapsules, the evaluation of repair efficiency, and the testing of microcapsule mechanical indexes. The study of mechanical properties of microcapsules is limited to the field of polymer materials, and the whole self-healing system is not considered. To better evaluate the healing properties of asphalt material with self-healing microcapsule, researchers have studied the action characteristics between microcapsule and asphalt materials [8–10]. Sun et al. mechanically stirred the prepared MUF microcapsules into asphalt of 160°C and studied the properties of the capsule materials in high-temperature asphalt [11]. Zhang et al. mixed self-healing microcapsule into asphalt mixture according to different dosages and studied the effects of microcapsule materials on high and low-temperature performance and fatigue performance of asphalt mixture [12]. Al Mansoori et al. found that the cracking of asphalt mixture containing capsule returned to 52.9% of the initial strength, and the cracking of asphalt mixture without capsule returned to 14.0% of the initial strength at 20°C [13]. Su et al. used circular heating-cooling process tests and found that microcapsules still kept a stable state after an extreme temperature change simulating temperature change in the natural environment. Moreover, interface debonding phenomenon did not

appear. These results indicate that microcapsules can remain stable in the asphalt materials [14].

Some studies have focused on the healing ability of the asphalt itself after damage. Wang et al. [15] analyzed the effects of maintenance time, temperature, and mix type on their self-healing properties from a single factor using a four-point bending fatigue test and proposed evaluation indexes to quantify the healing effect. On top of that, Huang et al. [16] further investigated the effects of damage degree and asphalt modifier on the self-healing properties of the mix. Through asphalt binder strength tests, Lv et al. [17] found that the type and amount of modifier had a great influence on the healing ability of asphalt mastic, and the increase of modifier weakened the self-healing ability of asphalt and soft asphalt had better healing ability. In addition, several researchers have investigated the rupture mechanism and release process of self-healing microcapsules. Zhu et al. used multi-scale analysis and composite fracture mechanics to study the mechanical property requirements of micro-encapsulated materials in asphalt pavements and the rupture mechanism of microcapsules under the action of micro-cracks [18]. Moreno-Navarro et al. found that asphalt mixtures with macroscopic cracks are more sensitive to healing conditions, and the healing rate increases with the rise of healing temperature [19]. Moreover, the healing ability of matrix asphalt is higher than that of modified asphalt; however, the application of heating or external forces as healing techniques has a lower recovery rate at macroscopic damage, but Zhong used dissipative energy theory to study and found that the healing ability of polymer modified asphalt was higher than that of matrix asphalt [20]. Qiu et al. tested the healing ability of asphalt mixtures using elastic foundation beams and evaluated quantitatively based on strength recovery and crack width, and the results showed that delayed viscoelastic healing was the main reason for the narrowing of crack width, and viscous healing played a dominant role in prolonged or high-temperature conditions [21].

According to the above research, the interface of crack can be quickly healed due to adhesion of adhesives and cohesion of the materials. The solidified adhesive layer has certain strength [22–24]. The capsule-core materials of microcapsules successfully prepared are divided into diluter and adhesive. The light oil of rejuvenator is used as a diluter to improve flow deformation property of asphalt by adjusting the viscosity and colloid structure of asphalt and to improve its self-healing ability. The epoxy resin mixed with curing agent as a adhesive to quickly heal the fractured interface of the asphalt material through its own cohesive force. The solidified adhesive layer has a certain strength, which could reliably connect two interfaces, transfer stress, and resist damage [25–27]. It is necessary to study and develop new experiments and new indicators to evaluate the self-healing properties of asphalt materials containing microcapsules.

In this study, asphalt-rejuvenator-asphalt (ARA) and asphalt-epoxy resin-asphalt (AEA) models were first developed and used to study the healing behavior of asphalt and capsule-core materials using Materials Studio software. Also, the molecular cross-linking and simulated stretching were implemented using the Perl script. Then, the model of bi-plate DSR tests were designed and the model was used to characterize the self-healing properties of asphalt material. Finally, the healing indexes (HI_1 and HI_2) were evaluated to quantify the self-healing effect of rejuvenator and epoxy resin in asphalt materials. This study excluded the interference of capsule wall and compared the healing effect of two types of capsulate-core materials with two different mechanisms of action, which will provide theoretical guidance for the selection and use scenarios of microcapsule core materials.

2. Molecular Dynamics Simulation

2.1. Modeling. To study the self-healing effect of epoxy resin and rejuvenator on asphalt from molecular scale, two molecular models of asphalt-epoxy resin (with hardener)-asphalt (AEA) and asphalt-rejuvenator-asphalt (ARA) were established in this study using Materials Studio 2020, as shown in Figure 1. Among them, the asphalt model is the four-component AAA-1 model proposed by Li and Greenfield [28]. The molecular models of epoxy resin and curing agent are DGEBA and IPD molecules, respectively. The molecular model of the rejuvenator is shown in Figure 2.

2.2. Simulation Process. First, the 12-component molecules were introduced into the cubic box using the Amorphous cell module according to the AAA-1 model number, and the initial density was set to 0.1 g/cm^3. Then, the initial model was geometrically optimized in 10,000 steps. The optimized model was subjected to 500 ps of molecular diffusion under NVT ensemble. Finally, NPT simulations of 500 ps were performed on the asphalt model to approximate the actual density at 298.15 K (25°C). COMPASS II was chosen for all force fields during the simulation process.

The ratio of the number of DGEBA and IPD molecules is 1 : 2. AEA and ARA models were built using the Build layer function. Subsequently, 10,000 steps of geometry optimization were performed for both models. Then, the models were simulated at NVT for 500, 1000, 1500, and 2000 ps at a diffusion temperature of 293.15 K (20°C), respectively. In addition, the AEA model was subjected to molecular cross-linking of DGEBA and IPD using a Perl script to simulate the reaction of epoxy resin and curing agent, and the cross-linking process is shown in Figure 3.

2.3. Molecular Simulation Tensile Test. In this study, a Perl script was used to implement a model for direct stretching experiments. The healing effect of the AEA and ARA models was investigated by stretching the models. The stretched models were subjected to geometric optimization to obtain kinetic parameters, and the stretching process is shown in Figure 4. Finally, the stresses generated after stretching the models were counted to evaluate the healing effect.

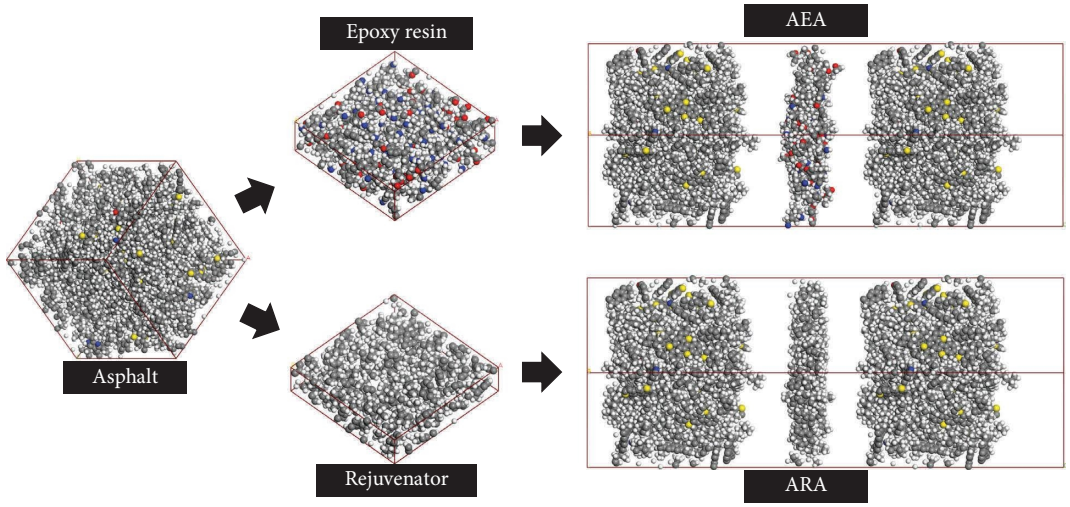

Figure 1: Schematic diagram of the modeling process of AEA and ARA models.

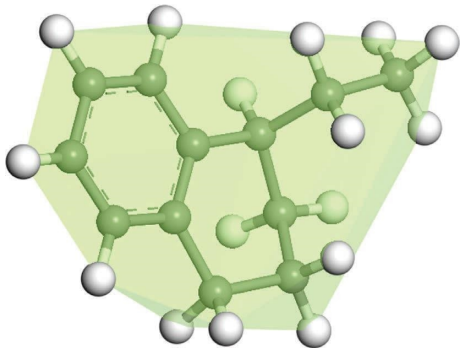

Figure 2: Molecular model of rejuvenator.

3. Materials and Experiments

3.1. Materials. SK-90# asphalt is selected as base asphalt. The proportion of the mineral powder and binders in the asphalt mortar is 1 : 1. The mineral powders are limestone fines (≤0.075 mm). The rejuvenator was produced by Zhuhai Jieda Petrochemical Trading Co. Ltd., and the composition is light oil containing aromatics and saturates. The adhesive was epoxy resin (DGEBA), and curing agent (IPD) was produced by Jining Hongming Chemical Reagent Co. Ltd. The composition of IPD is isophoronediamine ($C_{10}H_{22}N_2$). The major properties of raw materials are shown in Table 1. Figure 5 shows the three microcapsules prepared using three core materials. The research team studied the properties of the microcapsules and optimized the preparation process [27, 29].

3.2. Experimental Methods and Parameters. The rheological properties of asphalt binders and mastics under different temperatures, stresses, and strains were tested using DSR. The plates of both PP08 and PP25 were used under low and high-temperature conditions. Based on the DSR test, an experimental specimen was designed in this study to investigate the self-healing effect of the capsule-core materials in the asphalt materials. This specimen is mainly used to simulate the situation after rupture of microcapsule and release of core material. Firstly, the 0.003 g ± 0.0005 g capsule-core material (1.0% of asphalt content) is evenly applied between two asphalt specimens (10 mm in diameter and 2 mm thick) to prepare the bi-plate DSR tests, which formed a thickness of approximately 3.8 μm capsule-core material. The illustration of bi-plate DSR test and test samples is shown in Figure 6.

The asphalt-rejuvenator-asphalt specimens were placed in a constant temperature chamber at 20°C for 1–6 days. The asphalt-epoxy resin (with curing agent)-asphalt specimens were placed in a 20°C thermostat to heal for 6, 12, 18, and 24 hours, respectively.

The healing indexes (HI_1 and HI_2) were used to evaluate self-healing properties of asphalt materials, calculated as shown equations (1) and (2).

$$HI_1 = \frac{G^*_{healed}}{G^*_{original}}, \tag{1}$$

where G^*_{healed} is the initial dynamic shear modulus (Pa) of the bi-plate asphalt specimen and G^*_{original} is the initial dynamic shear modulus of the undamaged asphalt specimen.

$$HI_2 = \frac{N_{\text{healed}}}{N_{\text{original}}}, \tag{2}$$

where N_{healed} is the number of loading cycles of the bi-plate asphalt specimen when dynamic shear modulus drops to 50% of the initial value and N_{original} represents the corresponding loading cycles of undamaged asphalt specimen when dynamic shear modulus drops to 50% of the initial value.

Moreover, linear and exponential functions were used to fit the healing index based on dynamic shear modulus (HI_1) and fatigue life (HI_2), respectively. The fitting function used in this study was as shown in equations (3) and (4). The R^2 values of fitting functions were found in the range of 0.91–0.98, indicating the strong correlation.

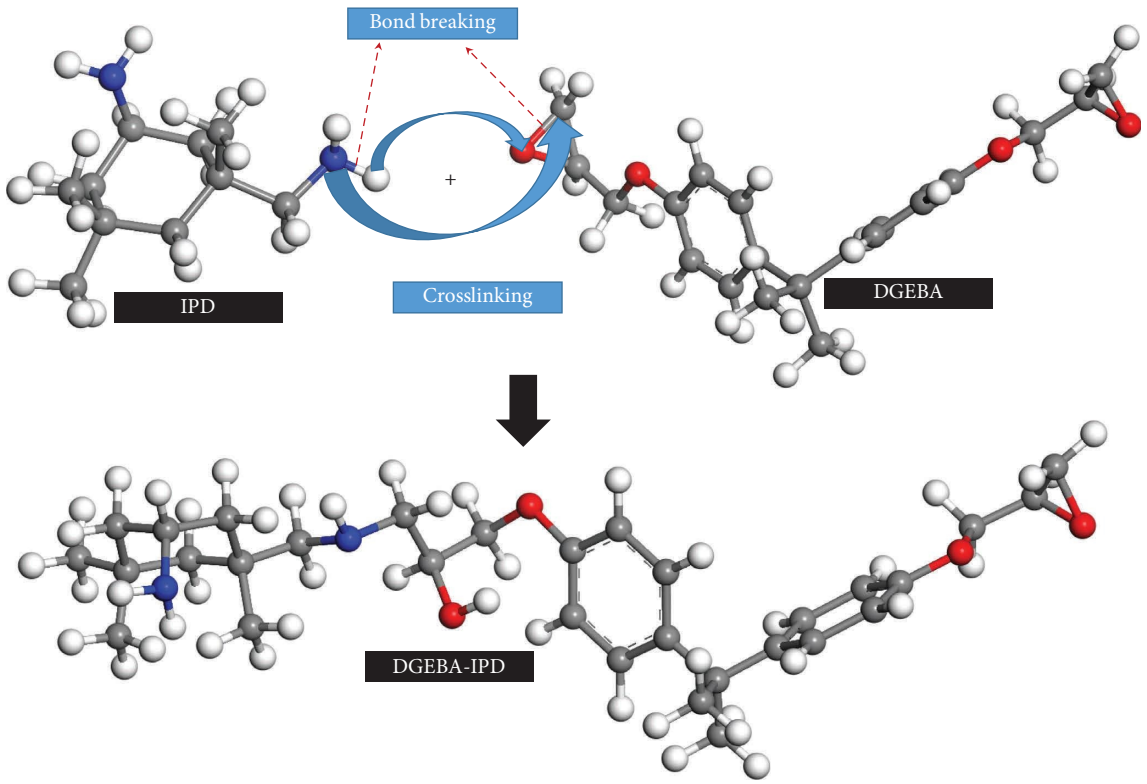

Figure 3: Cross-linking process of DGEBA and IPD molecules.

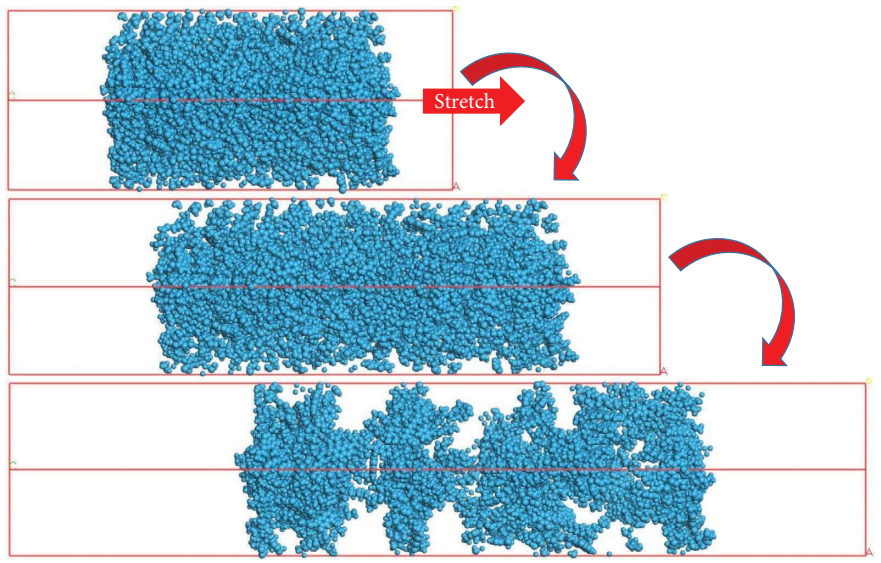

Figure 4: Stretching process of models.

Table 1: Major properties of raw materials.

Materials	Properties	Value
Asphalt	Penetration (25°C, 5 s, 100 g)/0.1 mm	89.2
	Softening point (ring & ball)/°C	45.1
	Ductility (5 cm/min, 15°C)/cm	>100
Epoxy resin	Epoxy equivalent (g/eq)	400–800
	Rotary viscosity (MPa·s, 25°C)	<1000
	Solid content (%)	50 ± 3

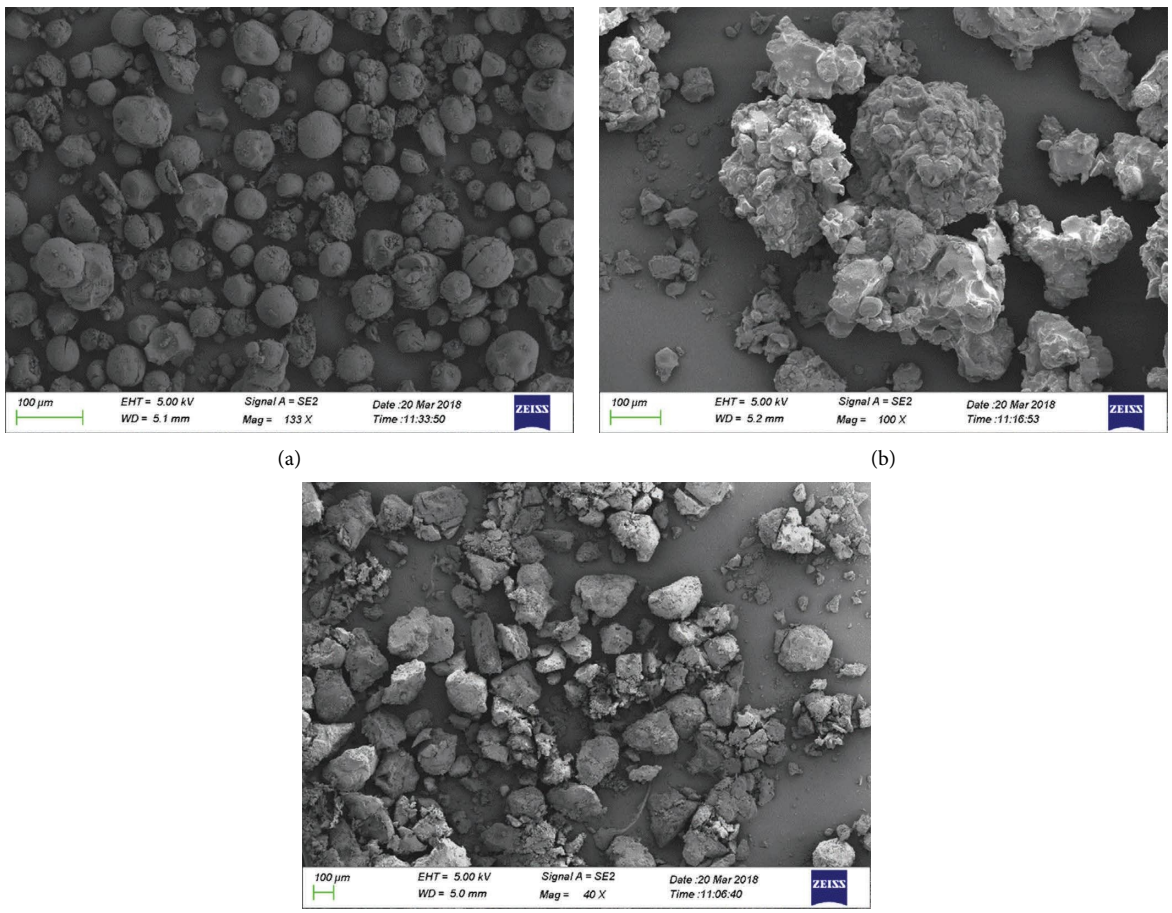

(a) (b)

(c)

Figure 5: Morphology of microcapsules: (a) DGEBA; (b) IPD; (c) rejuvenator.

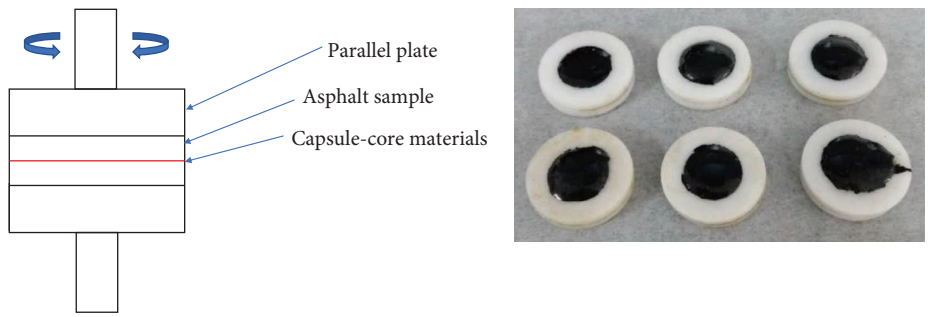

(a) (b)

Figure 6: Bi-plate DSR test: (a) illustration of test setup; (b) specimens.

$$y_1 = a_1 + b_1 t_1, \tag{3}$$

$$y_2 = a_2 e^{b_2 t_2}. \tag{4}$$

4. Results and Discussion

4.1. Comparison of the Healing Effect of Molecular Models

4.1.1. Cohesive Energy of Models with Various Simulation Times. The cohesive energy could be used to evaluate the cohesive properties of materials. A higher value of cohesive energy represents better intermolecular adhesion of the system. Therefore, the cohesive energy is used to evaluate the healing effect of rejuvenator and epoxy resin with asphalt. Figure 7 shows the ARA molecular model with different simulation times. The cohesive energy of the ARA and AEA systems was calculated according to equation (5). The calculated results are shown in Table 2 and Figure 8.

$$E_c = E_A + E_B - E_T, \tag{5}$$

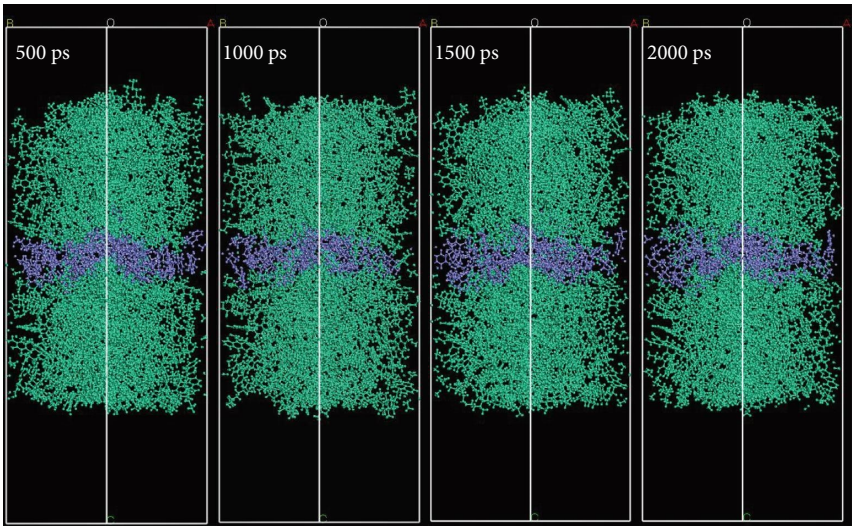

Figure 7: ARA molecular models with various simulation times.

Table 2: Energy of ARA and AEA models.

Model	Simulation time (ps)	Energy (kcal/mol)			
		Total	Rejuvenator/epoxy	Asphalt	E_c
ARA	500	18748.73	438.52	18937.47	627.26
	1000	18824.36	467.29	18990.29	633.23
	1500	18800.80	430.24	19030.88	660.32
	2000	18756.58	507.30	18912.06	662.79
AEA	500	9038.15	949.54	8911.56	822.95
	1000	8501.33	477.61	8903.83	880.11
	1500	8086.53	42.48	8915.32	871.27
	2000	7936.49	−147.99	8960.04	875.56

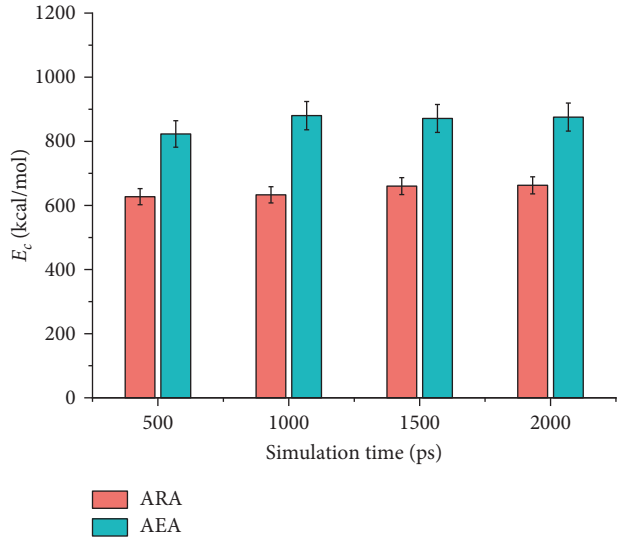

Figure 8: Cohesive energy of models with various simulation times.

where E_c is the cohesive energy of the model; E_A is the energy of the asphalt phase; E_B is the energy of the rejuvenator or epoxy phase; and E_T is the total energy of the system.

Figure 8 shows the cohesive energy results of ARA and AEA models for different simulation times. It can be seen from Figure 8 that the cohesive energy of AEA model is

larger than that of ARA under the same conditions, which indicates that the adhesion of epoxy resin and asphalt is better. With the increase of healing time, the cohesive energy of ARA model gradually increases while that of the AEA model increases first and then becomes stable. This reflects the slow healing process of the rejuvenator and the earlier strength of the epoxy resin. In terms of the healing mechanism, the rejuvenator heals mainly by promoting the diffusion of the asphalt itself, while the epoxy resin cures to increase the adhesion between the asphalt to achieve healing [27].

4.1.2. Stress of Models with Various Simulation Times. To further investigate the mechanical properties of the healed model, a Perl script was used to apply 50% strain to the model and count the stresses generated in the model after stretching for evaluating the healing effect. Figure 9 shows the AEA model after stretching. The statistical results of the stresses are shown in Table 3 and Figure 10. From Figure 10, it can be seen that the stress value of the ARA model is the highest at the healing time of 1500 ps. This indicates that the system has the highest strength at this time. This differs from the results for the cohesive energy. There are two possible reasons for this scenario: first, the experimental results are disturbed by the phenomenon of molecular chemical bond breakage that is not considered in the simulation of stretching [30]. Second, with the increase of diffusion time, the molecules of the rejuvenator gradually diffused into the asphalt interior causing the asphalt at the interface to become softer [31]. The stress value of the AEA model increases with the increase of the healing time. The model tensile state in Figure 9 also shows that the longer the healing time, the greater the degree of molecular cross-linking after stretching. This is basically the same as the actual epoxy curing process [32]. The stress values of the ARA model for the same simulation time are greater than those of the AEA model. It indicates that the ductility recovery of the material by the rejuvenator is better than that by the epoxy resin. Increasing the curing agent content will reduce the ductility of the epoxy resin material [33].

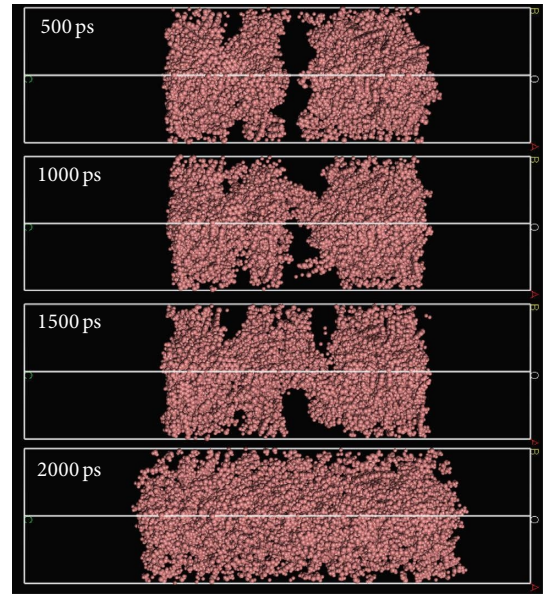

Figure 9: Stretched AEA models with various simulation times.

4.2. Rheological Properties of Asphalt Binder and Mastic

4.2.1. Temperature Sensitivity. The main control parameters of temperature sweep tests are shear strain of 0.1%, angular frequency of 5 rad/s, and heating rate of 2°C/min at −20–30°C. The main control parameters are shear strain of 1%, angular frequency of 10 rad/s, and heating rate of 2°C/min at 30–80°C. The test results of asphalt binders and mastics are shown in Figure 11.

As can be seen in Figure 11(a), the complex shear modulus ($G*$) of both asphalt binder and mastic increased briefly or remained flat during the initial warming phase. This may be due to the reorientation of molecules under the shear action. Also, the specimen thickness was 2 mm, and the temperature of the specimen could not rise uniformly for a short time, thus making the modulus rise briefly. However, after a gradual increase in temperature, the effect of temperature on the specimen is much greater than that of thickness, which leads to a gradual decrease in the modulus of asphalt and asphalt mastic with the increase in temperature. In Figure 11(b), $G*$ of asphalt binder and mastic gradually decreases with increasing temperature. In the initial stage, there is no similar situation as in the low-temperature results. This is probably due to the fact that the thickness of the asphalt specimen is 1 mm, and the temperature of the specimen changes more uniformly during the heating process, and the effect of temperature is much larger than the effect of specimen thickness. This also fully illustrates that asphalt binder and mastic are temperature-sensitive materials.

4.2.2. Stress-Strain Characteristics. The main control parameters of the stress scan are loading frequency of 10 Hz, test temperature of 20°C, and stress scan range of 0.01–1 MPa. The main control parameters of the strain scan are loading frequency of 10 Hz, test temperature of 20°C, and strain scan range of 0.01–100%. From Figure 12(a), it can be seen that $G*$ of asphalt mastic has been residing above the matrix asphalt at the beginning of the loading phase. With the gradual increase of shear strain, the modulus of the base asphalt and mastic began to decrease slowly, and then there was a sharp decline in the later stage, which was especially obvious for the asphalt mastic. The asphalt mastic specimens were the first to break than the base asphalt, showing a characteristic similar to brittle fracture, while the base asphalt broke relatively slowly. This indicates that the toughness of the base asphalt is higher than that of the asphalt mastic. From Figure 12(b), it can be seen that the property change pattern of base asphalt and mastic under stress scan mode is basically the same as that of the strain sweep test.

Table 3: Stress values of stretched models.

Model		Simulation time (ps)	Stress (MPa)		
			X-axis	*Y*-axis	*Z*-axis
ARA	Unstretched	500	26.77	9.99	69.91
		1000	126.91	91.40	160.89
		1500	17.28	42.22	12.93
		2000	−50.65	−7.85	39.09
	Stretched	500	49.40	54.52	15.09
		1000	55.80	58.17	21.76
		1500	76.09	58.89	69.90
		2000	51.96	58.72	58.72
AEA	Unstretched	500	77.05	69.63	6.56
		1000	70.10	60.17	7.32
		1500	78.25	75.98	6.90
		2000	74.07	81.31	7.31
	Stretched	500	44.18	51.26	15.07
		1000	48.02	43.50	15.10
		1500	51.83	45.15	19.67
		2000	58.16	54.08	34.68

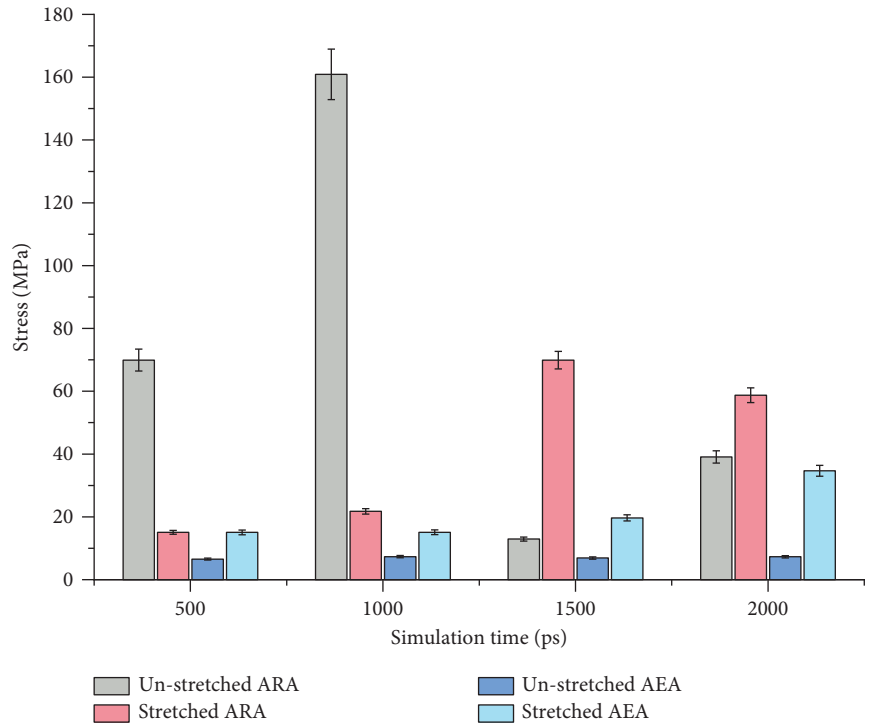

Figure 10: Stress results of models (*Z*-axis).

4.2.3. Fatigue Properties. The main control parameters of the fatigue test were temperature of 20°C and frequency of 10 Hz, and the asphalt specimens were subjected to fatigue tests with 0.1 MPa, 0.2 MPa, and 0.3 MPa shear stresses, respectively. The asphalt mastic specimens were fatigue tested with 0.2 MPa, 0.3 MPa, and 0.4 MPa shear stresses, and the results are shown in Figure 13. From Figure 13(a), it can be seen that for every 0.1 MPa increase in the control stress, $G*$ of the asphalt increases to some extent, but its fatigue life decreases by orders of magnitude. From Figure 13(b), it can be seen that the trend of $G*$ change of asphalt mastic is similar to that of asphalt binder, but its fatigue life decreases at a slower rate compared to that of asphalt binder. $G*$ of the asphalt binder specimen changes more slowly in the early stage and then decays faster when the specimen reaches a certain fatigue level. $G*$ of asphalt mastic decayed more uniformly in the early stage and more slowly in the later stage of damage. This indicates that the fatigue resistance of asphalt mastic is significantly better than the base asphalt [34].

4.3. Effect of Rejuvenator on Self-Healing. The DSR bi-plate specimens were prepared with rejuvenator and asphalt binder or mastic as raw materials and maintained at a

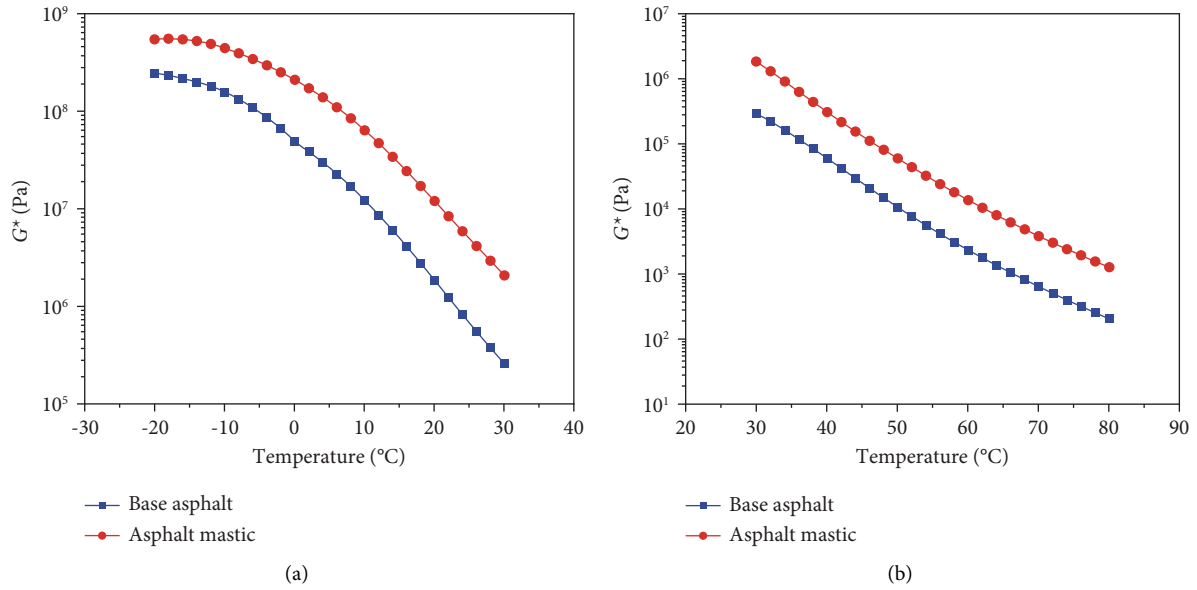

Figure 11: Complex shear modulus of asphalt materials: (a) −20–30°C; (b) 30–80°C.

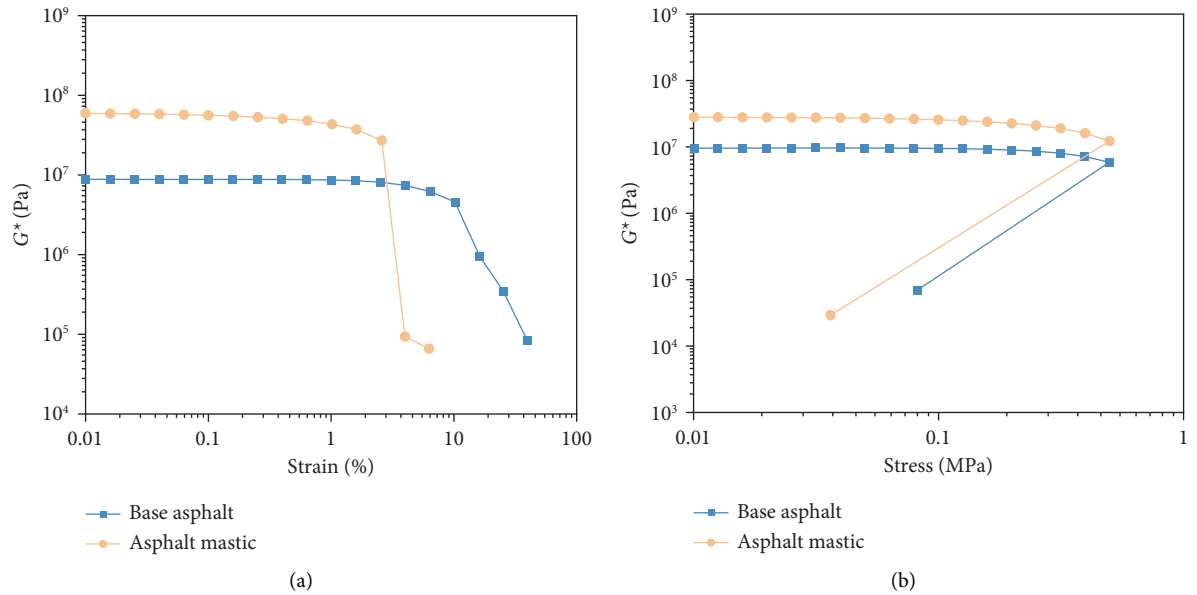

Figure 12: Complex shear modulus measured under different loading modes: (a) strains; (b) stresses.

constant temperature of 20°C for 1–6 days in an environmental chamber. The fatigue tests were performed sequentially. Figure 14 shows the fatigue test results of DSR biplate specimens at different stresses. Table 4 presents initial dynamic shear modulus of asphalt materials with rejuvenator at various stresses. It can be seen from Figure 14 and Table 4 that the initial modulus and fatigue life of the specimens increase with the extension of the curing time.

It can be seen from Figure 15(a) that HI_1 of the specimens gradually increased with the increase of the healing time. The healing index is influenced by the control stress, and the higher the control stress is, the higher the healing index is. When the control stress was 0.3 MPa, the healing index of specimens with healing time of 5 and 6 days exceeded 1. A healing index greater than 1 indicates that the introduction of the rejuvenator could not only heal the asphalt material but also improve the performance of the asphalt material. As shown in Figure 15(b), the HI_2 index of the specimens increased relatively slowly in the early stage but increased substantially in the later stage. HI_2 is also influenced by the control stress, and HI_2 of 0.3 MPa is always greater than the HI_2 value of 0.2 MPa. The healing index of 0.1 MPa is less than 0.3 MPa during the short-term healing time, but the growth rate of the healing index is much greater than 0.3 MPa when the maintenance time exceeds 4 days. Comparing Figures 15(a) and 15(b), it can be seen that the

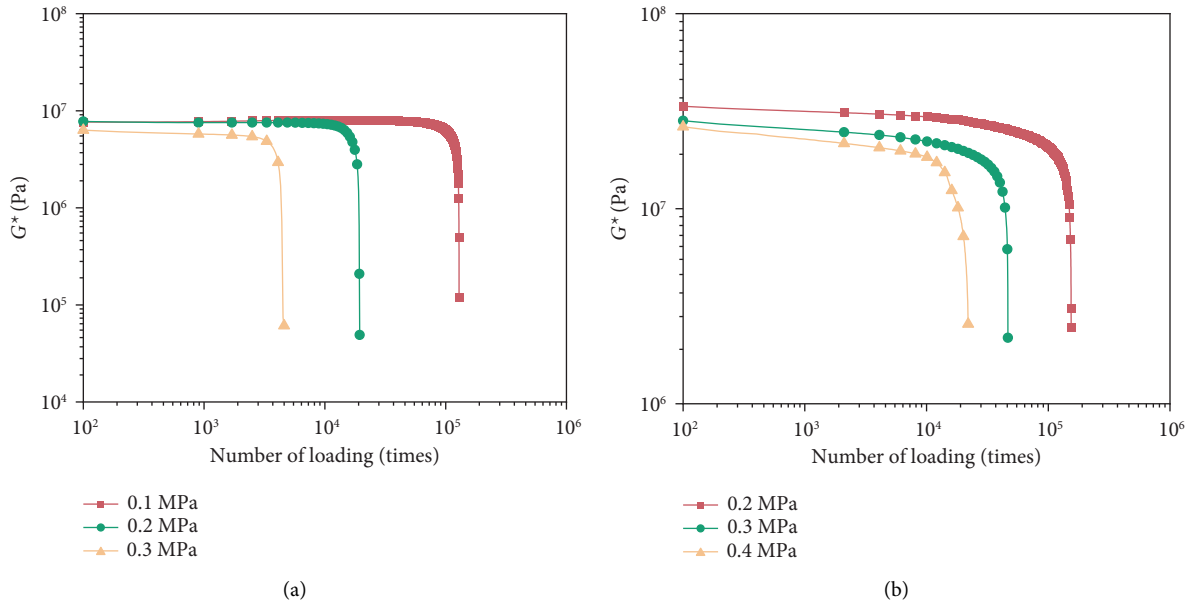

Figure 13: Fatigue testing results of undamaged samples: (a) binder; (b) mastic.

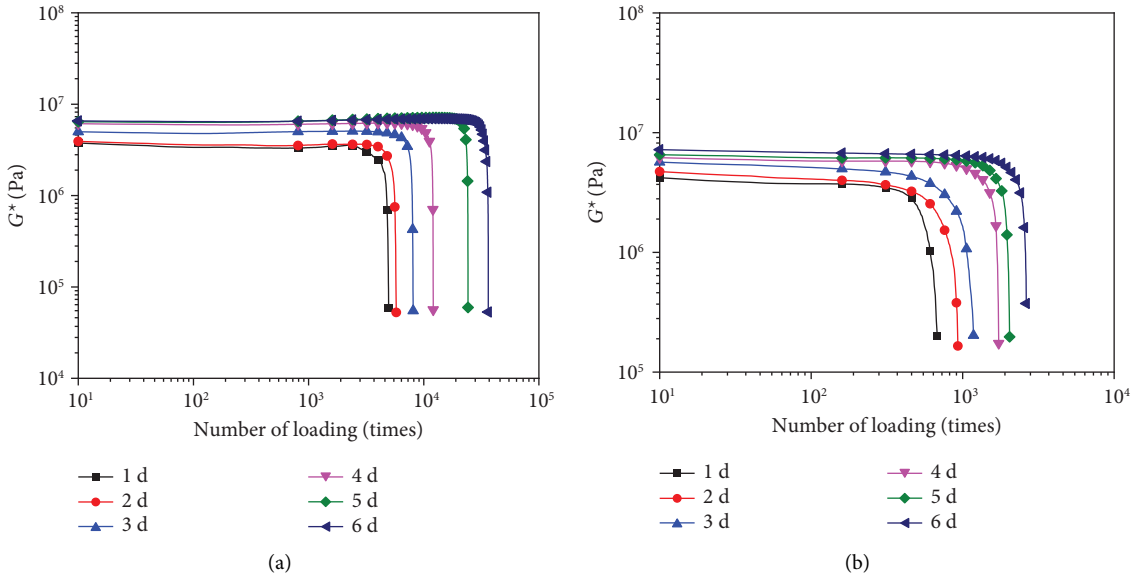

Figure 14: Continued.

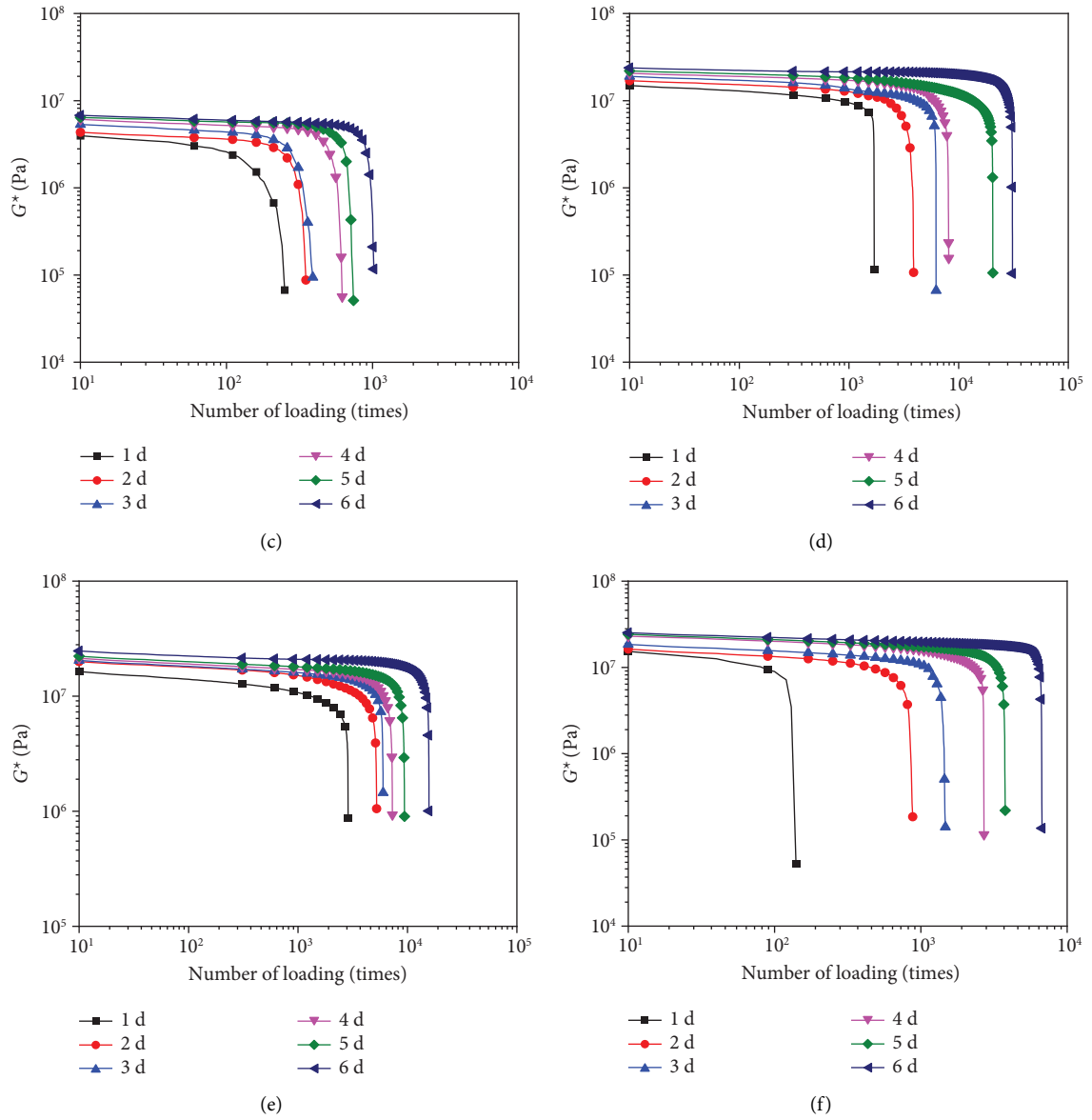

Figure 14: Fatigue testing results of healed samples with rejuvenator at various stresses: binder—(a) 0.1 MPa; (b) 0.2 MPa; (c) 0.3 MPa; mastic—(d) 0.2 MPa; (e) 0.3 MPa; (f) 0.4 MPa.

Table 4: Initial dynamic shear modulus of asphalt materials with rejuvenator at various stresses (MPa).

Sample	Stress (MPa)	Healing time					
		1 d	2 d	3 d	4 d	5 d	6 d
Binder	0.1	3.755	3.923	4.991	6.115	6.434	6.568
	0.2	3.962	4.337	5.325	6.096	6.408	6.799
	0.3	4.203	4.733	5.670	6.179	6.549	7.213
Mastic	0.2	14.909	16.97	18.995	2.0.594	21.962	23.767
	0.3	16.378	19.971	20.442	21.331	22.245	24.715
	0.4	25.265	22.970	24.241	15.304	16.283	18.493

healing index calculated by the modulus ratio is much larger than the healing index calculated by the number of loadings.

Similarly, HI_1 and HI_2 of asphalt mastic were calculated and the relationships between healing index and healing time are shown in Figure 16. The R-square values of fitting functions were found in the range of 0.90–0.99, indicating the strong correlation. The results indicate that self-healing properties of asphalt mastic and asphalt binder show consistent trends with healing time. It can be seen from Figure 16(a) that HI_1 of the specimens increased gradually

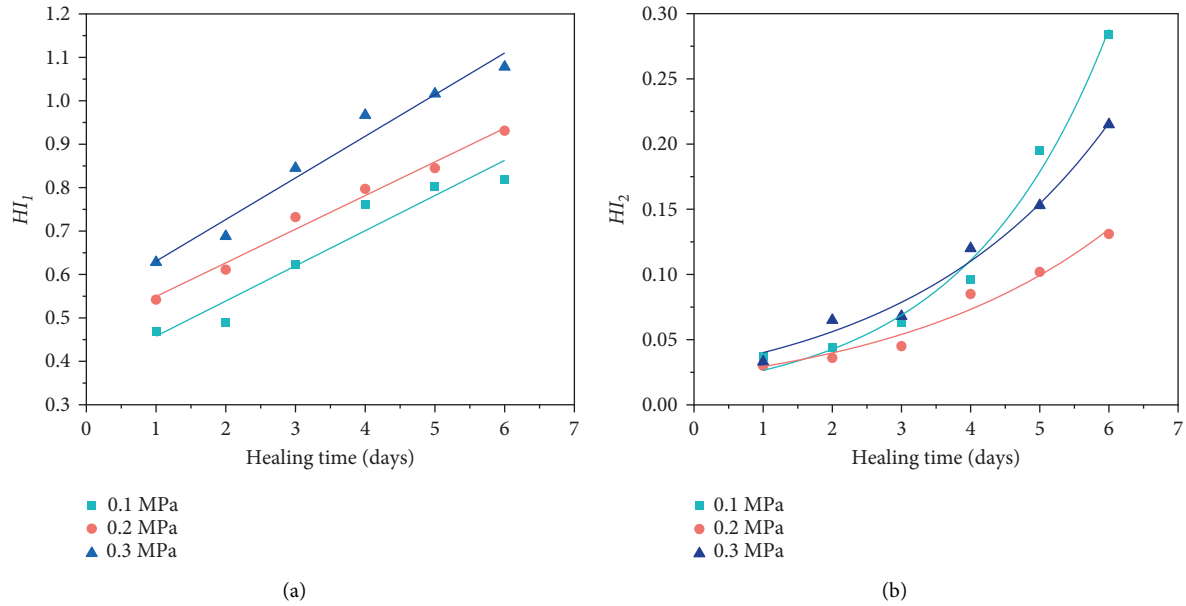

Figure 15: Healing index of asphalt binder with rejuvenator based on (a) dynamic shear modulus (HI_1); (b) fatigue life (HI_2).

with the growth of the maintenance time. The healing index HI_1 of the specimens was greater than 0.7 after 6 days. From Figure 16(b), it can be seen that HI_2 of the specimens grew exponentially, with a relatively slow growth in the early stage, but a burst growth in the later stage. HI_2 was also influenced by the test control stress. HI_2 of 0.2 MPa was always at the minimum value, and the healing index of 0.3 MPa was greater than 0.4 MPa during the short-term maintenance time. The healing index of 0.4 MPa increased faster and exceeded 0.3 MPa as the maintenance time was extended. This indicates that after the asphalt is damaged, the rejuvenator could heal it in a short period of time, but the damage location is still a weak surface of the whole, which can be easily destroyed under repeated loading, and the recovery of its fatigue performance is a long-term process. Comparing the healing index results of the rejuvenator on the binder and the mastic, the healing index value of the slurry is greater than that of the binder under the same test conditions. This indicates that the self-healing effect of the rejuvenator on the binder is more obvious [31].

4.4. Effect of Epoxy Resin on Self-Healing. The DSR bi-plate specimens of epoxy resin were maintained in an environmental chamber at 20°C for 6, 12, 18, and 24 hours and then subjected to fatigue tests. The fatigue test results of the asphalt binder and mastic specimens at the control stress of 0.2 MPa are shown in Figure 17. Table 5 presents initial dynamic shear modulus of asphalt materials with epoxy resin at various stresses. It can be seen from Figure 17 that the initial modulus and fatigue life of the specimens increase with the extension of the curing time under the same control stress condition.

Figure 18 shows the fitted curve of healing index of asphalt binder specimens. It can be seen from Figure 18(a) that the healing index HI_1 of the bi-plate specimens gradually increased with the increase of the curing time. The healing index HI_1 was greater than 1.0 after 24 hours. Under the conditions of control stress of 0.2 MPa and 0.3 MPa, the healing index HI_1 was greater than 1.0 after healing for 18 hours. Also, the healing index was influenced by the control stress; the greater the control stress, the higher the measured healing index. When the healing index is greater than 1, the introduction of the adhesive can not only heal the asphalt material but also improve the performance of the original asphalt material. From Figure 18(b), it can be seen that the healing index HI_2 of the specimens grows in a linear manner. Comparing Figures 18(a) and 18(b), the healing index calculated by the initial complex shear modulus ratio is much larger than that calculated by the number of loadings, which indicates that the binder can heal the asphalt in a short period of time after the asphalt has been damaged [35].

Figure 19 shows the fitted curve of healing index of asphalt mastic specimens. It can be seen from Figure 19(a) that the healing index HI_1 of the specimens gradually increased with the increase of the curing time under the conditions of control stress of 0.2 MPa and 0.3 MPa. On the contrary, the healing index HI_1 gradually decreases with the increase of the curing time under the condition of the control stress of 0.4 MPa. Under the condition of control stress of 0.4 MPa, the damage of the specimen was observed at the contact interface between the parallel plate and the specimen during the test, which belonged to the debonding between the specimen and the parallel plate, rather than the fatigue damage of the specimen itself; the two main reasons for this phenomenon were as follows: (1) the adhesion between the asphalt mastic itself and the parallel plate was small and the control stress was large during the test; (2) with the extension of the curing time, the epoxy resin cured to a higher degree. The degree of curing of the epoxy resin improves with longer maintenance time allowing the mechanical properties of the asphalt to recover and the specimen is easily debonded from the parallel plate under higher stress.

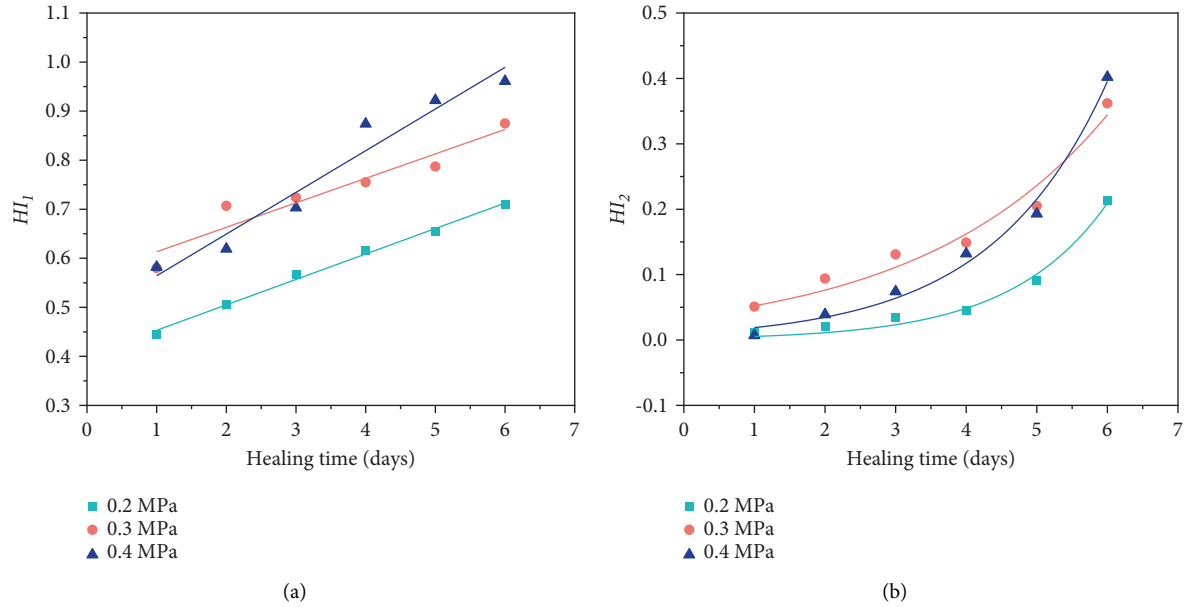

Figure 16: Healing index of asphalt mastic with rejuvenator based on (a) dynamic shear modulus (HI_1); (b) fatigue life (HI_2).

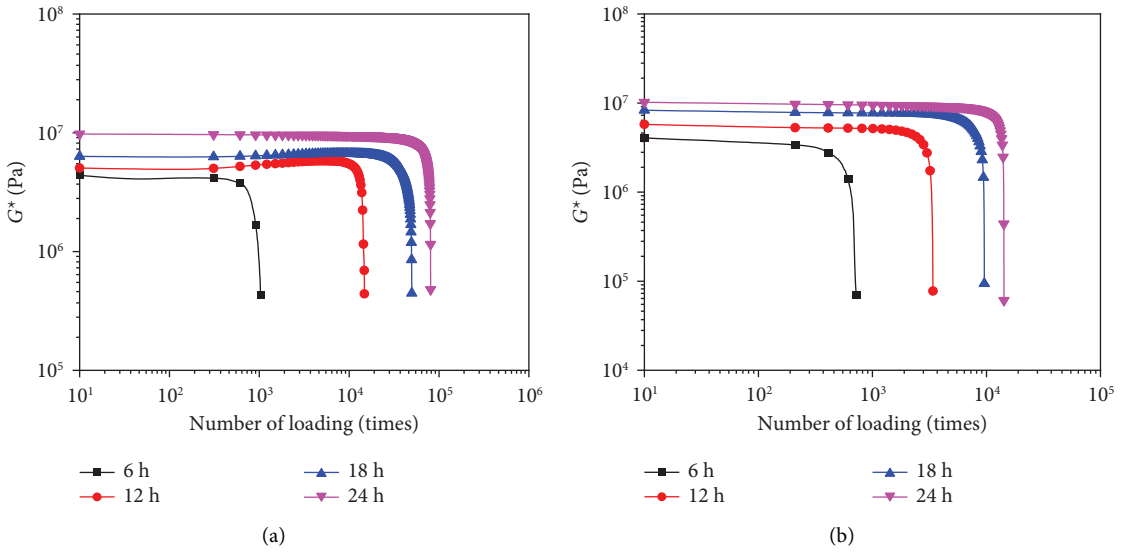

Figure 17: Continued.

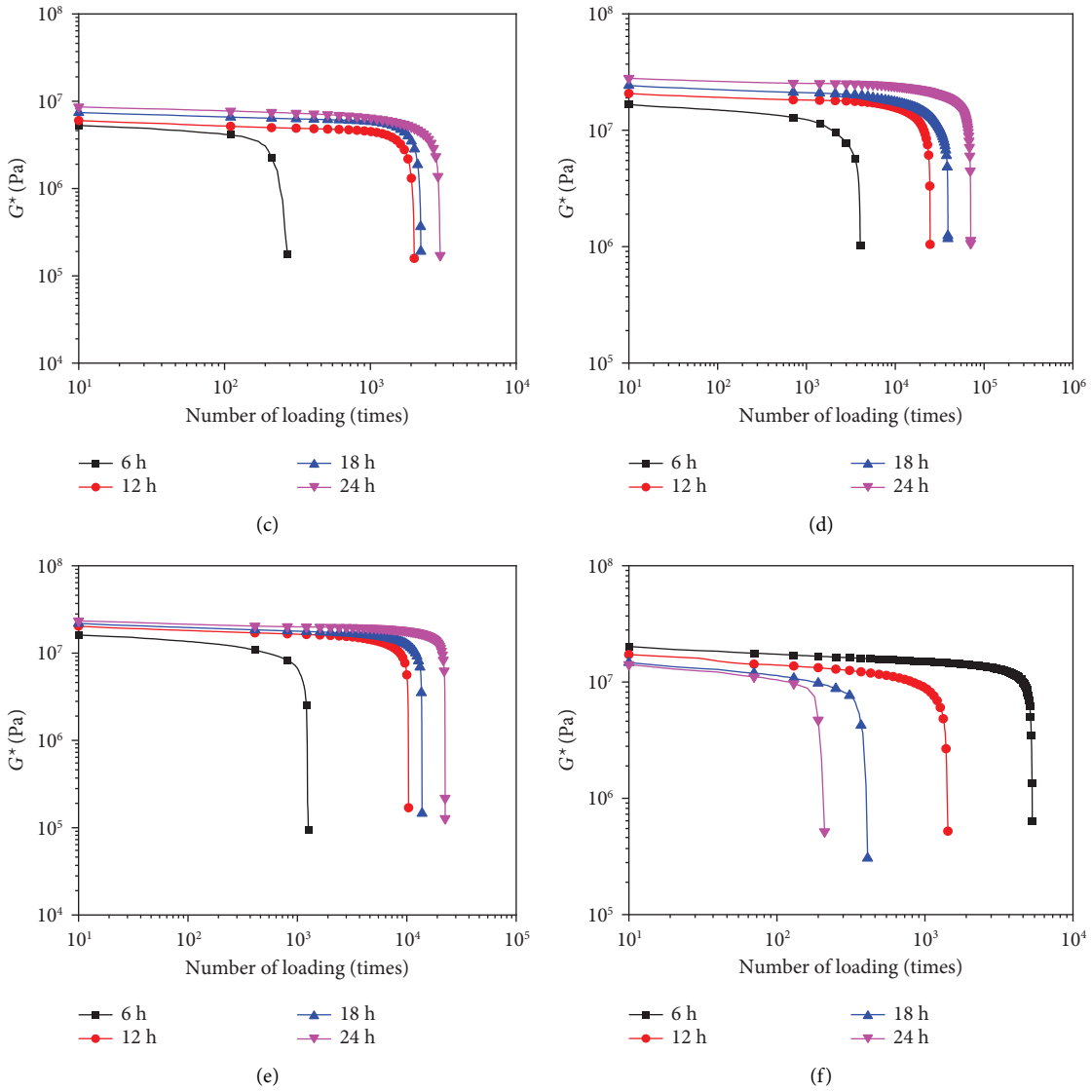

Figure 17: Fatigue testing results of healed samples with epoxy resin at various stresses: binder—(a) 0.1 MPa; (b) 0.2 MPa; (c) 0.3 MPa; mastic—(d) 0.2 MPa; (e) 0.3 MPa; (f) 0.4 MPa.

Table 5: Initial dynamic shear modulus of asphalt materials with epoxy resin at various stresses (MPa).

Sample	Stress (MPa)	Healing time			
		6 h	12 h	18 h	24 h
Binder	0.1	4.380	5.057	6.334	9.764
	0.2	4.055	5.768	8.303	1.019
	0.3	5.271	6.004	7.420	8.597
Mastic	0.2	16.635	20.696	24.225	27.975
	0.3	16.111	20.319	21.863	23.369
	0.4	20.194	17.209	14.702	14.138

Comparing Figures 19(a) and 19(b), it can be seen that the variation pattern of the healing index HI_2 of the two-piece specimen is basically the same as that of the healing index HI_1. The healing index HI_1 was greater than 0.8 and the healing index HI_2 was greater than 0.4 for the 24 h specimens under the control stress of 0.2 MPa and 0.3 MPa. The healing index calculated by the initial complex shear modulus ratio was much greater than that calculated by the number of loadings. This indicates that after the asphalt damage, the adhesive can make it heal in a short period of time, but fatigue damage is likely to occur under the action of repeated loading, and it takes a longer period of time to recover the fatigue performance.

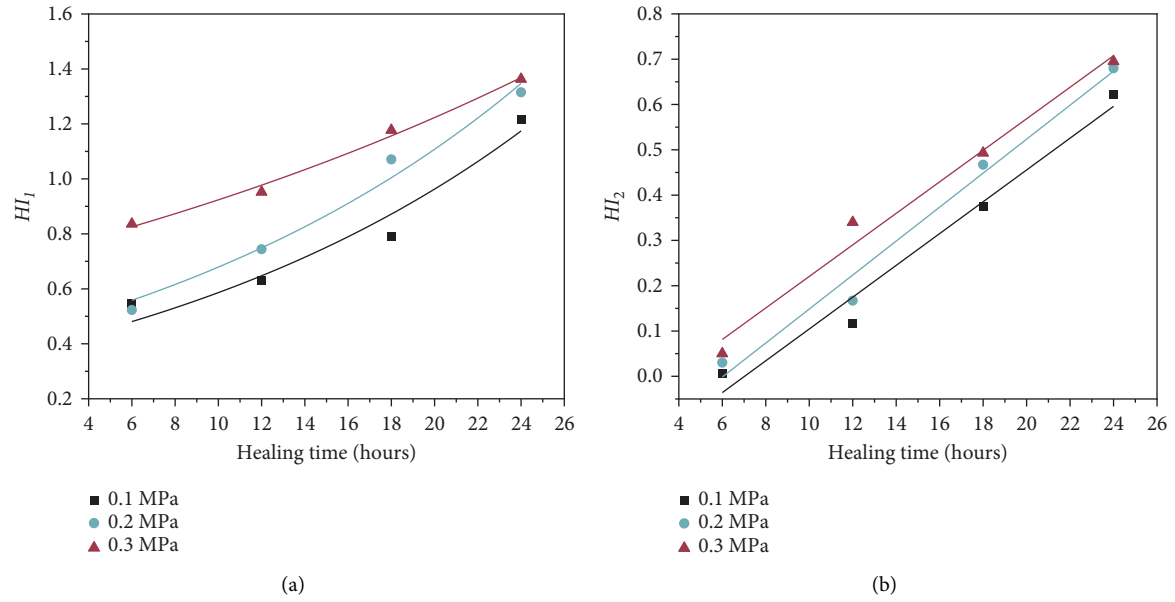

Figure 18: Healing index of asphalt binder with epoxy resin based on (a) dynamic shear modulus (HI_1); (b) fatigue life (HI_2).

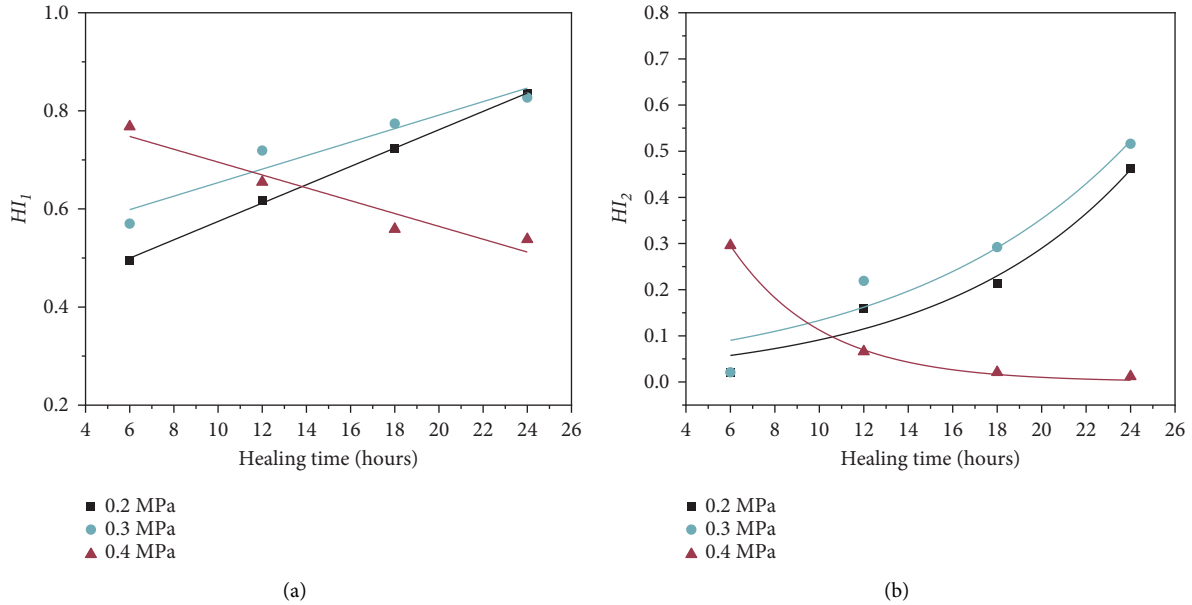

Figure 19: Healing index of asphalt mastic with adhesive agent based on (a) dynamic shear modulus (HI_1); (b) fatigue life (HI_2).

Comparing the healing index of epoxy resin to asphalt binder and mastic, the healing index value of asphalt binder is greater than that of asphalt mastic under the same conditions. This result indicates that the epoxy resin has a better healing effect on the asphalt binder different from rejuvenator. When the control stress was 0.3 MPa, the healing indexes HI_1 and HI_2 of the epoxy were greater than those of the rejuvenator, which indicated better self-healing of the epoxy. The value of HI_1 even

exceeded 1, which was due to the high strength of the cured epoxy [22]. This indicates that the epoxy resin material can better restore the shear strength of asphalt.

5. Conclusions

In this study, molecular dynamic simulations and rheological tests were used to investigate the effect of two capsule-core materials with various self-healing mechanisms such as rejuvenator and epoxy resin. The main conclusions are as follows:

(1) The epoxy resin has a stronger bond to the asphalt than the rejuvenator. This is due to the fact that the epoxy resin can be used as a binder while the main component of the rejuvenator is light oil according to the molecular simulation results. Importantly, the ARA model produced the highest stress after stretching. This indicates that the effect of the rejuvenator in restoring the ductility of the asphalt is promising.

(2) During the action of the rejuvenator and the asphalt material under the same controlled stress condition, the healing indexes HI_1 and HI_2 have a sound linear correlation with the maintenance time and the healing index HI_1 is much larger than HI_2, which indicates that after the asphalt is damaged, the rejuvenator can heal in a period of time. However, the damage position is still a weak point of the whole, which is easily destroyed under repeated loading, and the recovery of fatigue performance is a long-term process.

(3) Due to the high strength of the cured epoxy resin itself, the healed asphalt material has sound shear resistance. However, the amount of curing agent needs to be adjusted according to the actual situation.

(4) From the above results, the rejuvenator is recommended as microencapsulated materials for healing cracks due to temperature stress, while epoxy resin is more suitable for cracks due to vehicle load shear.

Data Availability

The data used to support the findings of this study are available from the corresponding author upon request.

Conflicts of Interest

The authors declare that they have no conflicts of interest.

Authors' Contributions

Suhua Chen was responsible for methodology, investigation, data curation, formal analysis, validation, original draft preparation, and review and editing. Qi Liu was responsible for conceptualization, software, review and editing, and supervision. Yanqiu Bi was responsible for original draft preparation, review and editing, and funding acquisition. Bin Yu was responsible for review and editing, supervision, and funding acquisition. Jiupeng Zhang was responsible for review and editing and validation.

Acknowledgments

This study was supported by the Jiangsu Transportation Science and Technology Project (grant no. 2020Y19-1(1)), National Natural Science Foundation of China (grant no. 5220082882), and Natural Science Foundation of Chongqing (grant no. 2022NSCQ-MSX1939). The authors greatly appreciate National Demonstration Center for Experimental Road and Traffic Engineering Education (Southeast University) in Nanjing, China.

References

[1] G. Fu, Y. Zhao, G. Wang, and J. Wei, "Evaluation of the effects of transverse cracking on the falling weight deflectometer data of asphalt pavements," *International Journal of Pavement Engineering*, vol. 23, no. 9, pp. 3198–3211, 2022.

[2] Z. Han, A. Sha, L. Hu, and L. Jiao, "Modeling to simulate inverted asphalt pavement testing: an emphasis on cracks in the semirigid subbase," *Construction and Building Materials*, vol. 306, Article ID 124790, 2021.

[3] X. Z. Cun, Q. Jin, and N. Zhang, "Experiment on permeability model and water stability of damaged asphalt mixture," *China Journal of Highway and Transport*, vol. 27, no. 3, pp. 1–10, 2014.

[4] W. Du, J. Yu, S. Gu et al., "Effect of temperatures on self-healing capabilities of concrete with different shell composition microcapsules containing toluene-di-isocyanate," *Construction and Building Materials*, vol. 247, Article ID 118575, 2020.

[5] Y. F. Zhu and H. L. Zhang, "Review of self-healing capacity of asphalt," *Materials Review*, vol. 29, no. 23, pp. 86–91, 2015.

[6] H. Shi, T. Xu, P. Zhou, and R. Jiang, "Combustion properties of saturates, aromatics, resins, and asphaltenes in asphalt binder," *Construction and Building Materials*, vol. 136, pp. 515–523, 2017.

[7] H. Shi, T. Xu, and R. Jiang, "Combustion mechanism of four components separated from asphalt binder," *Fuel*, vol. 192, pp. 18–26, 2017.

[8] M. R. Kessler, N. R. Sottos, and S. R. White, "Self-healing structural composite materials," *Composites Part A: Applied Science and Manufacturing*, vol. 34, no. 8, pp. 743–753, 2003.

[9] H. M. Jonkers, A. Thijssen, G. Muyzer, O. Copuroglu, and E. Schlangen, "Application of bacteria as self-healing agent for the development of sustainable concrete," *Ecological Engineering*, vol. 36, no. 2, pp. 230–235, 2010.

[10] Y. Yuan, M. Rong, and M. Zhang, "Preparation and characterization of poly(melamine-formaldehyde) walled microcapsules containing epoxy," *Acta Polymerica Sinica*, vol. 008, no. 5, pp. 472–480, 2008.

[11] D. Sun, Q. Pang, and X. Zhu, *Enhanced Self-Healing Process of Sustainable Asphalt Materials Containing Microcapsules*, Acs Sustainable Chemistry & Engineering, Washington, DC, 2017.

[12] L. Zhang, Q. Liu, and S. Wu, "Effects of self-healing capsule on road performance of asphalt mixture," *Journal of Wuhan University of Technology:Transportation Science & Engineering*, vol. 42, no. 1, pp. 39–43, 2018.

[13] T. Al-Mansoori, R. Micaelo, I. Artamendi, J. Norambuena-Contreras, and A. Garcia, "Microcapsules for self-healing of asphalt mixture without compromising mechanical performance," *Construction and Building Materials*, vol. 155, pp. 1091–1100, 2017.

[14] J. F. Su, S. Han, Y. Y. Wang et al., "Experimental observation of the self-healing microcapsules containing rejuvenator states in asphalt binder," *Construction and Building Materials*, vol. 147, pp. 533–542, 2017.

[15] H. P. Wang, J. Yang, and Z. Wang, "Investigation of fatigue and self-healing characteristics of asphalt mixtures," *Modern Transportation Technology*, vol. 11, no. 4, pp. 1–5, 2014.

[16] W. D. Huang, B. L. Li, and M. Huang, "Evaluation of self-healing of asphalt mixture through four-point bending fatigue test," *Journal of Building Materials*, vol. 18, no. 04, pp. 572–577, 2015.

[17] Q. Lv, W. Huang, and F. Xiao, "Laboratory evaluation of self-healing properties of various modified asphalt," *Construction and Building Materials*, vol. 136, pp. 192–201, 2017.

[18] Y. F. Zhu, X. Z. Zhao, and C. D. Si, "Mechanical analysis and fracture mechanism of self-healing microcapsules in asphalt pavement," *Materials Reports*, vol. 36, no. 10, pp. 44–49, 2022.

[19] F. Moreno-Navarro, P. Ayar, M. Sol-Sánchez, and M. C. Rubio-Gámez, "Exploring the recovery of fatigue damage in bituminous mixtures at macro-crack level: the influence of temperature, time, and external loads[J]," *Road Materials and Pavement Design*, vol. 18, pp. 293–303, 2017.

[20] J. H. Zhong, "Study on fatigue and self-healing characteristics of asphalt binder based on dissipative energy theory," *Highways & Automotive Applications*, no. 04, pp. 87–92, 2015.

[21] J. Qiu, A. A. A. Molenaar, M. F. C. van de Ven, S. Wu, and J. Yu, "Investigation of self-healing behaviour of asphalt mixes using beam on elastic foundation setup," *Materials and Structures*, vol. 45, no. 5, pp. 777–791, 2012.

[22] L. Yuan, J. Xie, G. Liang, L. Li, and J Guo, "Preparation and characterization of poly(urea-formaldehyde) microcapsules filled with epoxy resins," *Polymer*, vol. 47, no. 15, pp. 5338–5349, 2006.

[23] L. Yuan, G. Z. Liang, J. Q. Xie, L. Li, and J. Guo, "The permeability and stability of microencapsulated epoxy resins," *Journal of Materials Science*, vol. 42, no. 12, pp. 4390–4397, 2007.

[24] L. Yuan, G. Z. Liang, J. Q. Xie, J. Guo, and L. Li, "Thermal stability of microencapsulated epoxy resins with poly(-urea–formaldehyde)," *Polymer Degradation and Stability*, vol. 91, no. 10, pp. 2300–2306, 2006.

[25] R. Li, C. Wang, P. Wang, and J. Pei, "Preparation of a novel flow improver and its viscosity-reducing effect on bitumen," *Fuel*, vol. 181, pp. 935–941, 2016.

[26] B. Xue, H. Wang, J. Pei, R. Li, J. Zhang, and Z. Fan, "Study on self-healing microcapsule containing rejuvenator for asphalt," *Construction and Building Materials*, vol. 135, pp. 641–649, 2017.

[27] Q. Liu, J. P. Zhang, W. L. Liu et al., "Preparation and characterization of self-healing microcapsules embedding waterborne epoxy resin and curing agent for asphalt materials," *Construction and Building Materials*, vol. 183, pp. 384–394, 2018.

[28] D. D. Li and M. L. Greenfield, "Chemical compositions of improved model asphalt systems for molecular simulations," *Fuel*, vol. 115, pp. 347–356, 2014.

[29] W. Liu, J. Zhang, Q. Liu, J. Pei, C. Zhu, and P. Liu, "Effects of emulsifier dosage and curing time on self-healing microcapsules containing rejuvenator and optimal dosage in asphalt binders," *Journal of Nanoscience and Nanotechnology*, vol. 19, no. 1, pp. 57–65, 2019.

[30] X. Zheng, W. Xu, K. Cao, and K. Li, "Self-healing behavior of recycled asphalt prepared by residue oil of straw liquefaction based on molecular dynamics simulation," *Scientific Reports*, vol. 12, no. 1, p. 2718, 2022.

[31] D. L. Kuang, W. C. Liu, and Y. Zhang, "Evaluation of interface diffusion behavior between rejuvenator and aged asphalt based on surface wettability theory," *China Journal of Highway and Transport*, vol. 33, no. 07, pp. 58–67, 2020.

[32] M. Li, Z. Min, Q. Wang, W. Huang, and Z. Shi, "Effect of epoxy resin content and conversion rate on the compatibility and component distribution of epoxy asphalt: a MD simulation study," *Construction and Building Materials*, vol. 319, Article ID 126050, 2022.

[33] M. Xu, J. Yi, D. Feng, Y. Huang, and D. Wang, "Analysis of adhesive characteristics of asphalt based on atomic force microscopy and molecular dynamics simulation," *ACS Applied Materials & Interfaces*, vol. 8, no. 19, pp. 12393–12403, 2016.

[34] G. Liu, D. Han, Y. Jia, and Y. Zhao, "Asphalt mixture skeleton main force chains composition criteria and characteristics evaluation based on discrete element methods," *Construction and Building Materials*, vol. 323, Article ID 126313, 2022.

[35] Q. Liu, B. Yu, A. Cannone Falchetto, D. Wang, J. Liu, and W. Bo, "Characterization and molecular mechanism of the thermal-oxidative gradient aging behavior in asphalt films," *Measurement*, vol. 199, Article ID 111567, 2022.